Optical Fiber Technology 75 (2023) 103184

Contents lists available at ScienceDirect

Optical Fiber Technology

journal homepage: www.elsevier.com/locate/yofte

Demonstration of 200 Gbps PAM-4 transmission in a limited-bandwidth system using a two-tap THP with nonlinearity compensator

Seung-Woo Lee [a,*], Sang-Rok Moon [a], Hae Young Rha [b], Joon Ki Lee [a]

[a] Optical Network Research Lab, Electronics and Telecommunications Research Institute, 218 Gajeong-ro, Yuseong-gu, Daejeon 34129, South Korea
[b] MIROandI, Yuseong-gu, Daejeon, South Korea

A B S T R A C T

In this paper, we have proposed a digital signal processing (DSP) method for a 200 Gbps pulse-amplitude modulation level-4 (PAM-4) transmission in a bandwidth-limited system. To mitigate inter-symbol interferences (ISI) in the system and reduce the propagation of errors in the receiver, the Tomlinson-Harashima precoding (THP) technique was applied to the transmitter. For simplicity, the number of THP taps was limited to two (i.e., one coefficient to be optimized); the residual ISI resulting from the short tap was compensated for with a decision feedback equalizer (DFE). The performance of the proposed DSP was analyzed via experiments and simulations. Compared to conventional DSP techniques (such as DFE and the maximum likelihood sequence estimation (MLSE) without THP), the proposed DSP performs better within the limited-bandwidth region. As a result, the soft-decision forward error correction (SD-FEC) threshold (of 2×10^{-2}) was satisfied even when the bandwidth fell to below 35% of the baud rate. To enhance this performance, post-filter and MLSE were additionally applied, after which its performance was investigated. In addition, the nonlinear characteristics of the components were alleviated by applying a pre-distortion technique to the THP using look-up tables; this further enhanced performance, lowering the SD-FEC threshold's bandwidth to 32% of the baud rate.

1. Introduction

Data traffic associated with cloud network services and between data centers are increasing and require a lot of bandwidth, and recent studies related to 200 Gbps-class-transmission-*per*-lambda report high throughput and are used in short-reach links [1–4]. Compared to coherent communication, the intensity modulation/direct detection (IM/DD) format of communication is the most competitive modulation scheme in short-reach optical transmission systems due to their low levels of cost, complexity, and power consumption. This scheme typically includes various modulation formats such as the pulse amplitude modulation (PAM), discrete multi-tone (DMT), and carrier-free amplitude phase modulation (CAP). Amongst them, PAM4 has become the most widely adopted solution for gigabit ethernet (GbE) applications [5].

When transmitting 200 Gbps of PAM-4 signals, one of the most important issues is compensating for the inter-symbol interference (ISI) incurred through channels whose bandwidths are limited. To mitigate ISI while improving performance and cost-efficiency, various digital signal processing (DSP) techniques have been proposed for application in narrow-bandwidth systems [2,6,7]. To thus utilize DSP at the receiver, the use of a feed forward equalizer (FFE) has been proposed along with a feedback equalizer (FBE) or a maximum likelihood sequence estimator (MLSE). However, when ISI becomes a serious concern, the signal suffers from noise-enhancement and error-propagation. To solve these issues, the FFE-based equalizer was incorporated on the receiver side with a post-filter before MLSE to suppress the equalization enhancement noise [6–7]. Similarly, on the transmitter side, a combination of the Tomlinson-Harashima precoding (THP) technique (as a pre-equalizing method) and receiver-side FFE or MLSE has been proposed. When the THP is used as a transmitter-side pre-equalizer of the decision feedback equalizer (DFE), error-propagation can be avoided. The system preprocessed by THP with 33 GHz bandwidth limitations demonstrates experimental PAM-4 transmissions at 94 GBaud [2]. Although the THP performed remarkably better in the limited-bandwidth system, it uses a large number of filter taps [8–10], which complicates their optimization. In addition, the long path delay in the filter of the THP may cause problems with the timing of the critical path during hardware implementation. To overcome these obstacles, reducing the number of THP taps may be helpful.

In this paper, we have explored the DSP techniques applicable to bandwidth-limited IM/DD systems by employing a two-tap THP at the transmitter to reduce error propagation. In the receiver, in addition to the conventional FFE, the FBE is used to alleviate any residual ISI and share the receiver's burden of the equalization function with THP at the transmitter. Commonly used DSPs, such as DFE and MLSE (without

* Corresponding author.
E-mail address: beewoo@etri.re.kr (S.-W. Lee).

https://doi.org/10.1016/j.yofte.2022.103184
Received 28 December 2021; Received in revised form 7 November 2022; Accepted 27 November 2022
Available online 10 December 2022

THP), were compared with the proposed DSP with 200 Gbps of PAM-4 transmission over 10 km. The performance and limitations of the proposed DSP in bandwidth-limited situations were analyzed via experiments and simulations. Here, the bandwidth limitation was simulated by adding a low-pass filter (LPF) to the receiver. As a result, when the bandwidth falls to below 35% of the baud rate, the proposed scheme is demonstrated in this paper to improve performance over the existing combination of DFE and MLSE. It is also shown that the soft-decision forward error correction (SD-FEC) limit is satisfied in the 35 GHz bandwidth (35% of baud rate) of the 200 Gbps PAM-4 signals. To investigate the possibility of further improvement, we added advanced DSP techniques — such as MLSE with post-filter and nonlinear compensation — to this structure and studied their impacts with experimental and simulations.

The upcoming section proposes the DSP structure and the experimental setup of the 10-km-long, limited-bandwidth fiber transmission of the 200 Gbps PAM-4 signals are presented in the third section, while its results are analyzed and discussed in the next section. To further improve the performance of this system, we have applied and studied post-filters, MLSE, and nonlinearity compensators in our systems; the results of these are depicted in the fifth section. This is followed by our concluding remarks.

2. Overall DSP architecture

Fig. 1(a) and (b) depict the functional DSP block in the transmitter and receiver, respectively. In the transmitter, the data stream was generated using the pseudo-random bit sequence (PRBS) pattern, and the pattern length was 2^{15}-1. The pseudo-random data was mapped in the form of a PAM-4 signal in gray code. In addition, training symbols were sent to train the channel equalizer of the DSP receiver, after which the data symbols were transmitted. The two-tap THP was used after generating the PAM-4 symbol in the transmitter. The output of two-tap THP encoder was then oversampled with two samples per symbol. It was also pre-emphasized to equalize the frequency responses of radio frequency (RF) amplifier, modulator, and the digital to analog converter used in the arbitrary waveform generator (AWG). Following this, the signal was shaped by a raised cosine (RC) filter having a roll-off factor of 0.01 at the transmitter.

Coming to the DSP architecture of the receiver, the receiver obtained 160 GSa/s of signals from a digital sampling oscilloscope (DSO) with 59 GHz of analog bandwidth and 8-bit resolution. These signals were resampled with two samples per symbol and shaped by the RC filter with a roll-off factor of 0.1. After this, LPF was used in a gray box to simulate its performance and its bandwidth was changed to determine its performance in various structures at different bandwidths. We then estimated the start of the frame and cross-correlated it to determine the starting position of the data stream. Following this, the data was delivered to a timing synchronizer consisting of an error estimator, error compensator, and a loop filter. This included the use of the Gardner algorithm to detect and estimate timing errors and a second-order loop filter (with $k_1 = 0.0005$ and $k_2 = 5 \times 10^{-6}$) to stabilize the timing recovery loop. After this, the signal was delivered to the DFE consisting of 130 taps of FFE and 10 taps of FBE with T/2 symbol intervals. The coefficients of the DFE were updated by the least mean squares (LMS) algorithm at a rate of 0.0002. After the symbols were equalized in DFE, the output of the FFE was connected to the MLSE with two of memory length.

2.1. Simple two-tap THP and DFE to compensate for residual ISI

Since the existing THP uses a DFE coefficient value optimized for channel response, a large number of filter taps have been generally used as described before. In addition, the filter coefficients of the THP are obtained from the training-symbol-aided DFE, which uses LMS method to update the coefficient value of feedback filter, which have a value equal to or less than a decimal point. In the two-tap THP, the filter coefficient is determined by one decimal place from the coefficient of first-tap in FBE. For example, if the filter coefficient values of the FBE are optimized to {0.6022 0.12055 0.11391–0.0034117 …} in the case of DFE + MLSE, the two-tap THP has fixed value of 0.6 as the optimal filter coefficient. However, this paper adopts a two-tap THP, which has the following advantages over the existing THP. First, the two-tap THP does not require accurate channel estimation and feedback and second, the complexity associated with its designs is very low.

However, to configure pre-equalization with only two taps, the

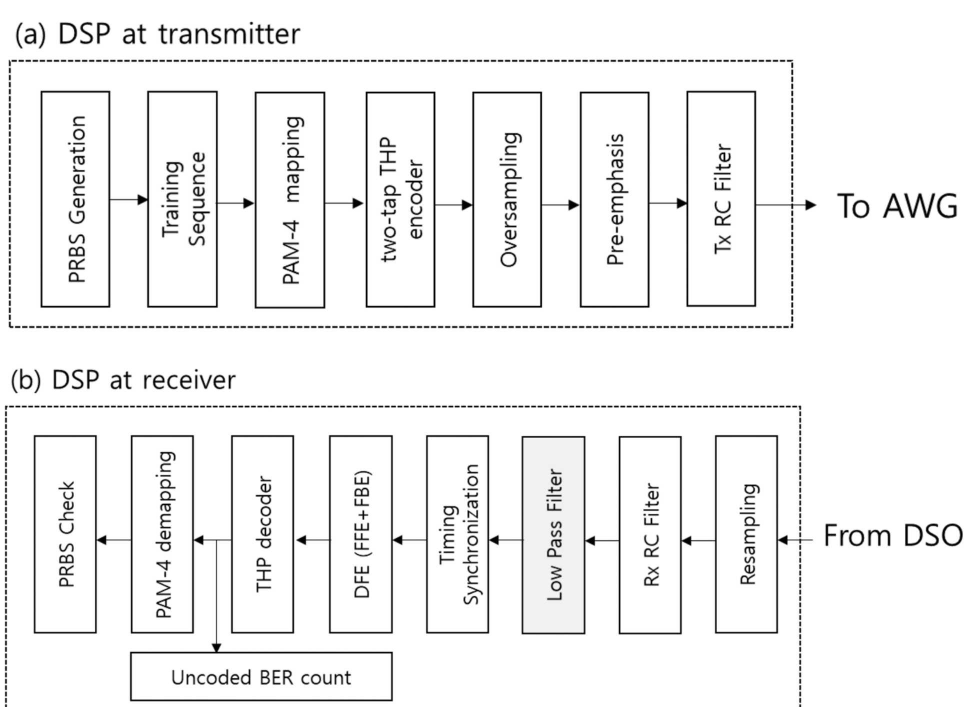

Fig. 1. Overall architecture of (a) transmitter DSP, and (b) receiver DSP.

feedback coefficient of the DFE is still required to alleviate the residual ISI, as shown in Fig. 2. The FBE operates with a two-tap THP having a fixed coefficient in the actual channel to adaptively compensate for any post-cursor ISI that may be caused. Therefore, the value of the FBE coefficient represents the difference between the filter coefficients of the two-tap THP and the required channel equalizer. In addition, when the received symbols of the FBE are erroneous, the overall bit errors may include some degree of error propagation. In this regard, by selecting a sufficient coefficient value for ISI removal using the above technique, the FBE coefficient can be kept small and the effect of error propagation can be alleviated.

3. Experimental setup

The experimental setup is shown in Fig. 3. To drive the O-band Mach-Zehnder modulator (MZM), an electrical, 200 Gbps, PAM-4 signal was generated by the offline transmitter, in combination with 120 GSa/s of the AWG with 8-bit resolution and 45 GHz of analog bandwidth. The signal generated by the AWG was modulated by the MZM of the transmitter and then transmitted through 10 km of single-mode fiber (SMF), after which its received optical power (ROP) was adjusted using a variable optical attenuator. We used a positive-intrinsic-negative photodiode with a bandwidth of 50 GHz, used RF amplifiers on the electrical signals, and sampled them using 160 GSa/s of 8-bit DSO with an analog bandwidth of 59 GHz. The samples were demodulated with an offline receiver and the wavelength of the optical signal was 1310 nm. Fig. 3 shows the frequency spectrum of the received signal from the offline receiver, especially the signal from the RC filter for the case of with or without THP based on the LPF bandwidth.

4. Results and discussion

4.1. THP coefficient optimization

In general, DFE alone (or the DFE + MLSE combination) is widely used to eliminate ISI. For this purpose, we adopted two-tap THP and DFE with coefficients to share the equalization functions with the transmitter and receiver while performing as well as the DFE does. In environments involving the transmission of 200 Gbps of signals with the PAM-4 format across lengths of over 10 km while maintaining sufficient bandwidth, we seek to determine two aspects:

i. the variation in bit error rate (BER) measurement results, and
ii. the best-performing structure amongst DFE, DFE + MLSE and THP + DFE.

In DFE + MLSE, the BER of the MLSE was measured when the output of the FFE, not hard-decision value but equalized signal, was input to the MLSE [11]. In MLSE, the branch metric is calculated using the input value of MLSE (output signal value of FFE) and the accumulated path metric through the trellis is obtained from employing the Viterbi algorithm. After tracing back the trellis states, the most probable data sequence is decoded. To compare their performances, THP + DFE and DFE + MLSE were made to have the same number of feedforward and feedback coefficient taps optimized in DFE.

We first study how BER varies with the THP coefficient for all three structures (THP + DFE, DFE, and DFE + MLSE), determine its optimal value (i.e., the coefficient value at which BER is minimized), and compare this variation across all three structures. Fig. 4 is a graphical depiction of this comparison; it summaries the 10-km-long optical-fiber-transmission performances of the structures at 59, 35, and 30 GHz of the LPF bandwidth. By changing the THP coefficient value from 0.1 to 0.9 by 0.1, the BERs of both DFE and MLSE were obtained for each structure. In the figure, the dotted blue line denotes DFE, while the solid blue line depicts DFE + MLSE; both blue lines depict structures without THP in 59 GHz of bandwidth. At all values of the coefficient, DFE + MLSE performs better than both THP + DFE and DFE. At a low THP coefficient (~0.1–0.2), the BERs of DFE and THP + DFE (at the same bandwidth of 59 GHz) are similar, while DFE performs better at higher levels of the coefficient (~0.8–0.9). A THP coefficient of approximately 0.6 was observed to be optimal for the THP + DFE structure, as its BER was the lowest at this point across all bandwidths. Our experiment showed that at a baud rate of 100 GBd, the transmitter had an analog bandwidth of 45 GHz of AWG and 45 GHz or more of the modulator, while DSO and PD had analog bandwidths of at least 50 GHz. Accordingly, the bandwidth of the overall system was sufficient to transmit 100 GBd PAM-4 signals [3]. For the experimental setup to have sufficient bandwidth in the system, the THP + DFE structure with the optimized two-tap THP coefficient should have a BER no greater than that of the HD-FEC threshold. In addition, even if the THP coefficient is low, BER below the hard-decision (HD)-FEC threshold may be adequate. Moreover, the DFE and DFE + MLSE structures performed similar to or better than THP + DFE with the optimized coefficient. THP + DFE with 0.6 of coefficient and DFE had BERs of 3.76×10^{-3} and 3.46×10^{-3}, respectively, with DFE + MLSE having the better BER of 1.27×10^{-3}. BERs of all three structures met below the HD-FEC threshold of 3.8×10^{-3}.

The above results were those of the case when the bandwidth was enough to transmit 200 Gbps of PAM-4 signals, whereas the following results are indicative of the system having poor bandwidth. We aim to determine how the performance of limited-bandwidth systems change for each structure. Therefore, we have swept the system bandwidth by adding LPF on simulation and setting its bandwidth. The location of the LPF in the simulation corresponds to the Rx RC filter, as shown in the gray box in Fig. 1. In this paper, a 5th-order Butterworth filter was utilized to emulate the receiver bandwidth. In Fig. 4, for LPF bandwidths of 35 and 30 GHz, system BERs were measured with the THP coefficients for the THP + DFE, DFE, and DFE + MLSE structures. In the figure, black and magenta lines depict the DFE + MLSE and THP + DFE structures, respectively, while the solid lines with circles and asterisks indicate LPF bandwidths of 35 and 30 GHz, respectively. For the limited bandwidth, in case of coefficient of 0.5 or more in two-tap THP, the THP + DFE structure performs better than or similar to both DFE and DFE + MLSE. In particular, the coefficient obtained by achieving the optimal BER of THP + DFE is 0.6, which is the same as its optimal value at sufficient

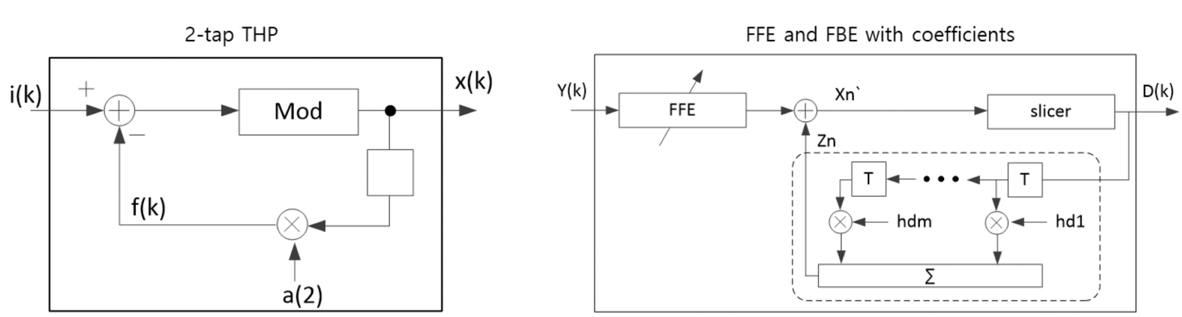

Fig. 2. Block diagram of two-tap THP and FFE and FBE with coefficients to compensate for residual ISI.

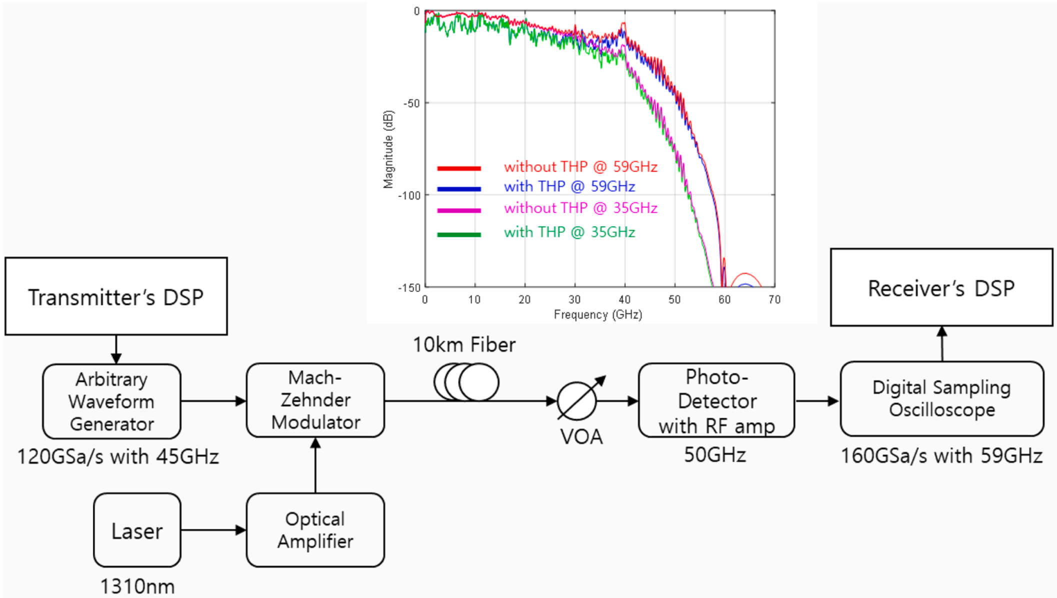

Fig. 3. Block diagram of the DSP experimental setup.

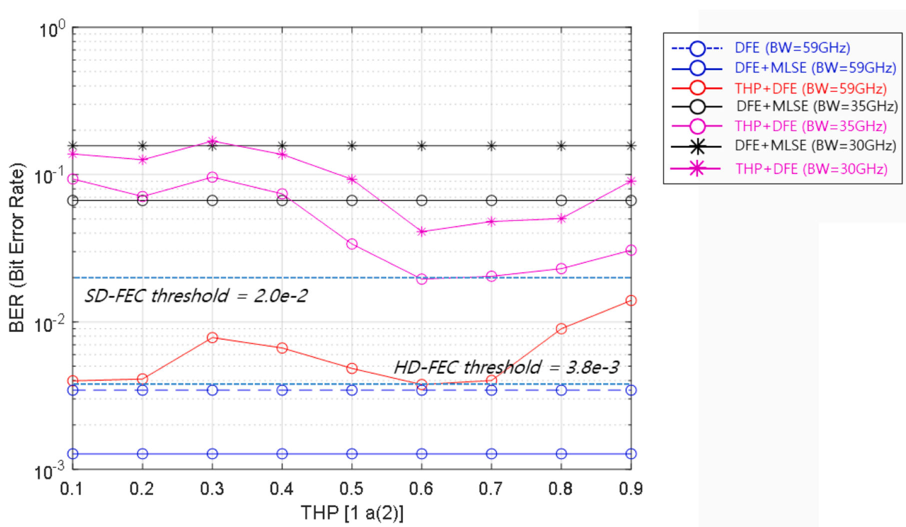

Fig. 4. Variation in BER with THP coefficients for the DFE, DFE + MLSE, and THP + DFE setups.

bandwidth. A BER of 1.76×10^{-2} was obtained to satisfy the SD-FEC threshold. Therefore, regardless of bandwidth, the coefficient value of 0.6 has an optimal BER in THP + DFE.

According to the experimental results of this paper, when the bandwidths of the LPF are 59 GHz and 35 GHz, the first filter coefficient of the FBE has an optimum value of 0.6 to 0.7, and thus the coefficient of the FBE does not change to a large step value. When the two-tap THP coefficient increases from 0.6 to 0.7, the level of the equalized signal also increases from 6 to 8. As the signal level increases, the SNR must increase to maintain the BER. Therefore, since the required SNR is larger than the gain obtained by increasing the THP coefficient to 0.7, the optimal performance can be achieved at 0.6 even in the bandwidth-limited system.

4.2. Experimental results of 200 Gbps transmission

We measured the performances of the THP + DFE, DFE, and DFE + MLSE structures for optical back-to-back transmission at 200 Gbps in the PAM-4 format across 10 km of fiber. Fig. 5 shows the relationship between ROP and BER for the aforementioned three structures under the given conditions. In it, THP0.6 indicates the two-tap THP technique with a fixed coefficient of 0.6. For all structures, the BER of optical back-to-back transmission is marginally better than that of 10 km of fiber transmission. With the DFE + MLSE, receiver sensitivity at the 7% overhead HD-FEC limit of 3.8×10^{-3} was about +2 dBm, whereas the same for the DFE and THP + DFE structures were +3 dBm, resulting in a signal-to-noise ratio (SNR) gain of about 1 dB. In the transmission experiments, the receiver's power was fixed at +3 dBm.

As we mentioned before, the effect of error propagation can be mitigated by reducing the occurrence of burst errors using a simple two-tap THP and DFE combination. Fig. 6(a) and (b) show the burst symbol errors for DFE and THP + DFE under conditions with similar BERs. In Fig. 6, the experimental conditions are the ROP value of +3dBm, 10-km-long fiber transmission, and THP having the coefficient of 0.6. In Fig. 6 (a), DFE has some burst symbol errors, while in Fig. 6(b), many burst symbol errors have disappeared. Therefore, when the THP coefficient was set to a value close to optimization, error propagation was almost alleviated.

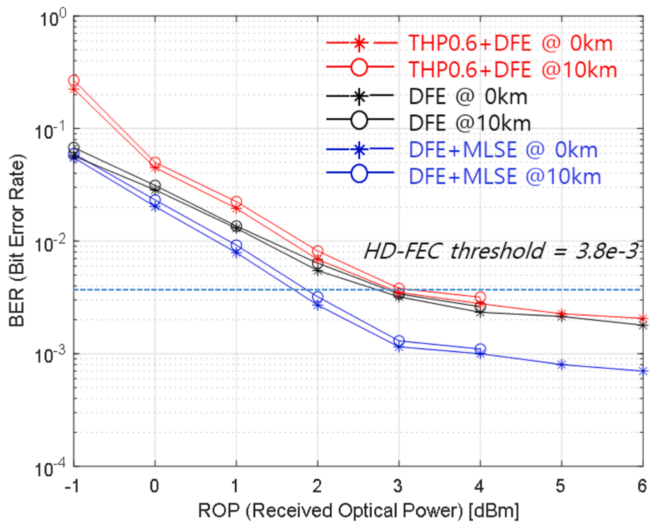

Fig. 5. Relationship between ROP and BER during optical back-to-back and 10-km-long fiber transmission with the THP + DFE, DFE, and DFE + MLSE structures.

4.3. Effects on bandwidth limitation

In Fig. 7, the THP coefficient is kept at 0.6 and, while varying the LPF's bandwidth, we studied the BER performance of the systems for cases of sufficient and insufficient bandwidth. According to the graphical results, when the LPF bandwidth does not exceed 40 GHz and when there is no THP, the THP + DFE has a lower BER than do the DFE and DFE + MLSE structures, whereas the DFE + MLSE structure performs better than THP + DFE when the bandwidth exceeds 40 GHz. As the LPF bandwidth decreased, the THP + DFE structure performed better than DFE and DFE + MLSE. Additionally, the lower the LPF bandwidth, the larger difference in the BERs of the systems. In other words, using THP may result in better performances in a situation where bandwidth is insufficient. During the simulation, THP + DFE and DFE required a bandwidth of at least 50 GHz to satisfy the HD-FEC threshold, but the

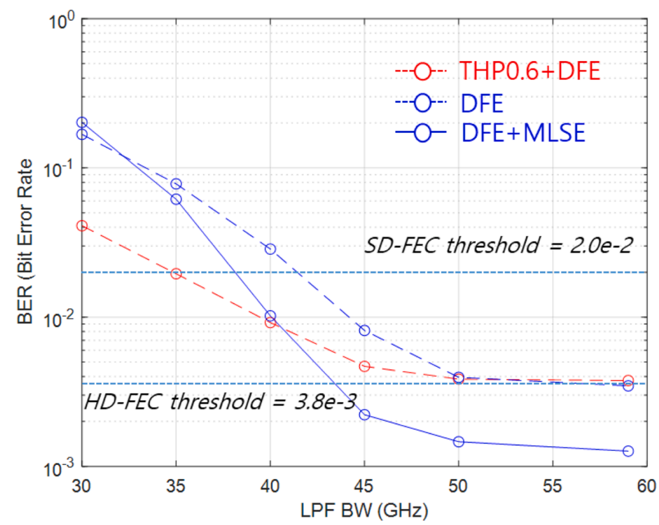

Fig. 7. Relationship between BER and LPF bandwidth for the THP + DFE, DFE, and DFE + MLSE structures.

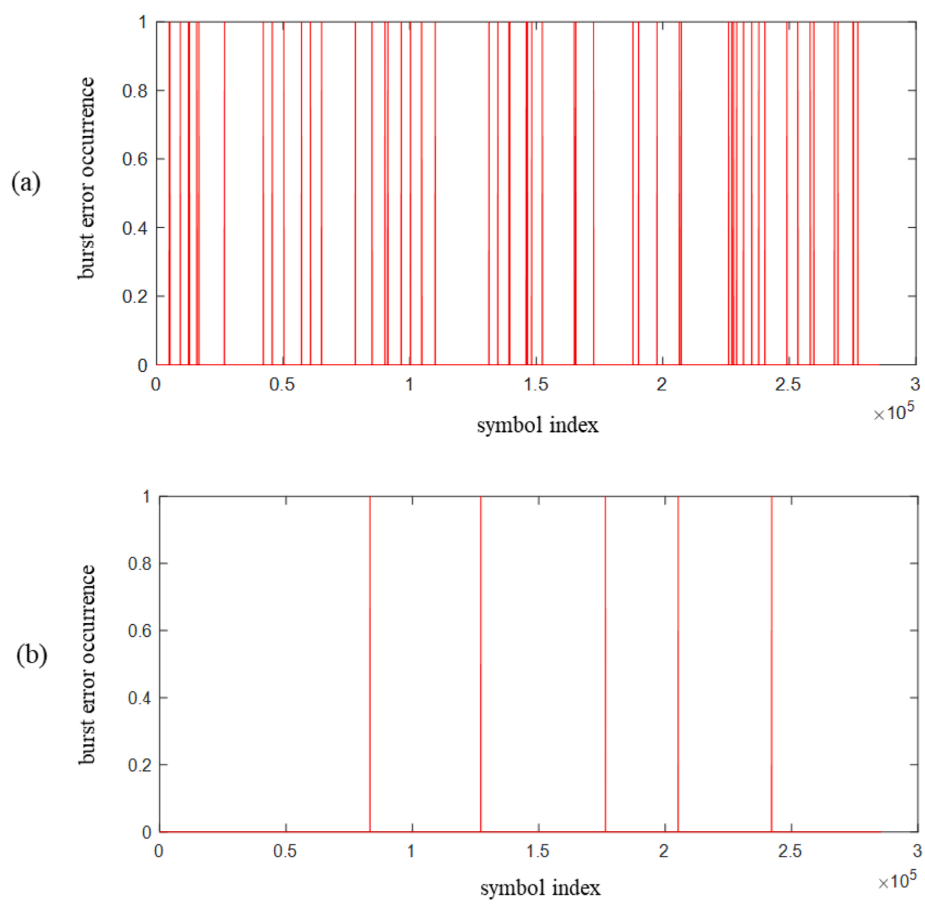

Fig. 6. Burst symbol errors in (a) DFE, and (b) THP + DFE structures.

minimum bandwidth to achieve BER below 20% of the overhead SD-FEC threshold (of 2.0×10^{-2}) was approximately 35 and 42 GHz, respectively. In DFE + MLSE, the HD-FEC threshold is satisfied even at a bandwidth of 43 GHz, but it should have a bandwidth of about 38 GHz to achieve BER below SD-FEC threshold. It can be seen that the lower the bandwidth, the better the THP + DFE's BER performance over DFE and DFE + MLSE.

5. Improvement with post-filter + MLSE and nonlinearity compensation

5.1. DSP architecture with post-filter + MLSE and nonlinear, two-tap THP

In this paper, since the symbol rate is at a high speed of 200 Gbps, performance gets degraded not only due to bandwidth limitations but also due to nonlinear effects. The nonlinearity effects in the IM/DD systems induced by electro-optical modulator and square-law detection in the photo-detector also limit the overall system performance. A nonlinear pre-distortion technique based on look-up tables (LUT) is an effective way to overcome these problems and deal with nonlinearity effects [12–13]. In this paper, the information on the correction values of nonlinear characteristics is stored in LUT-based memory according to each level of the received signal and is implemented in a transmitter. In the THP + DFE structure, based on the value of the THP coefficients, the signal level received through the DFE is four or more. When the bandwidth is inadequate, the signal levels may range from six to eight and should be applied according to the level received to the DFE. Therefore, in this paper, we apply the nonlinear correction value based on the equalized signal level before the THP decoder rather than the signal level of the THP decoder output. The nonlinear correction value is then accumulated and its mean chosen, and then updated to the LUT level of the THP nonlinearity compensator. Fig. 8(a) shows the block diagram of the modified THP with the LUT-based pre-distortion applied to it. To further enhance its performance, the BER was measured by adding MLSE to the two-tap THP and DFE described in the previous section. In addition to the 16-state MLSE with two of memory length, the two-tap post-filter was included to suppress equalizer enhancement noise [7]. Fig. 8 (b) and (c) show the nonlinear THP encoder and the post-filter + MLSE included in the modified DSP architecture as a gray box. The THP + DFE + post-filter + MLSE structure was configured by connecting the slicer output of the DFE to the MLSE.

5.2. Optimization of THP coefficient

After applying post-filter + MLSE to the THP + DFE structure, we measured its optimized coefficient and compared the enhancement in its performance due to this addition. Fig. 9 shows the relationship between

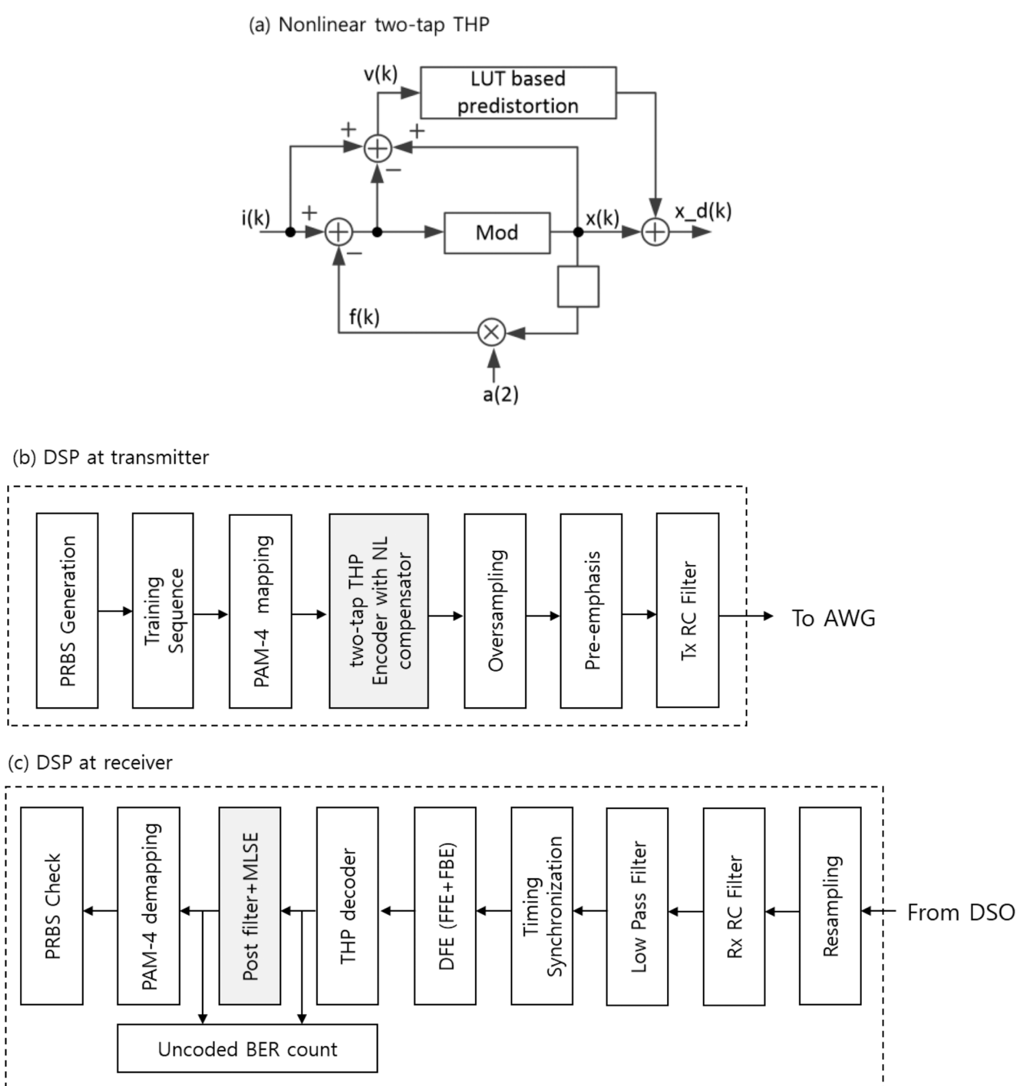

Fig. 8. Block diagram of the nonlinear, two-tap THP and modified DSP architecture with post-filter + MLSE.

BER and the coefficients of the THP + DFE and THP + DFE + post-filter + MLSE structures at LPF bandwidths of 59, 35, and 30 GHz. When MLSE is added to the THP + DFE combination, the amount of ISI eliminated varied as the THP coefficient was close to the filter coefficient of the optimized FBE, obtained from the channel inverse response. We chose a fixed value close to the first feedback filter coefficient. In case of low THP coefficients in conjunction with the THP + DFE + post-filter + MLSE structure, the BER of the MLSE was significantly improved over that of the DFE structure — this can be attributed to the greater robustness of MLSE against ISI. However, when the THP coefficient is high, the mitigating effect of ISI and, accordingly, the ISI-resistant properties of MLSE, varies with the value of the THP coefficient — as the THP coefficient increases, the BER improvement effect by MLSE weakens. However, the BER results of DFE are further improved due to the ISI phenomenon mitigated by THP as the THP coefficient approaches the optimized value of the channel response. After DFE, applying post-filter + MLSE suppresses the equalization-enhanced noise and improves BER performances [7]. As can be seen from Fig. 9, regardless of the LPF bandwidth, the optimized THP coefficient was 0.6. In particular, for low bandwidths of 35 and 30 GHz, low coefficient values (0.1–0.2) had worse BERs than did the optimized coefficient of 0.6.

For several DSP schemes in the paper, the hardware computational complexity was compared. In DFE, the hardware complexity calculates the number of adder and multiplier based on the filter's coefficients. THP is also calculated by the number of coefficients. In addition, in MLSE, adder and multiplier used by path metric calculation play an important role in complexity, and the PAM level and constraint length value becomes an important factor. Therefore, MLSE increases complexity a lot. From a hardware point of view, Table 1 shows the computational complexity comparison among these DSP structures.

5.3. 200 Gbps PAM-4 transmission over 10 km of fiber

We measured the performance when two-tap THP with nonlinearity compensator and post-filter + MLSE structures were included in THP + DFE. Fig. 10 shows the improved BER results when THP with nonlinear LUT-based predistortion in the transmitter and post-filter + MLSE in the receiver were applied while varying the LPF bandwidth. Therefore, the joint LUT pre-distortion and THP equalization for system nonlinear impairments can further improve performance. THP + DFE with nonlinearity compensator required a bandwidth of 45 GHz to satisfy the HD-FEC threshold, but the minimum bandwidth to satisfy the SD-FEC threshold was approximately 33 GHz. In the THP + DFE + post-filter + MLSE structure, the HD-FEC threshold was satisfied even at 38 GHz, but the SD-FEC threshold should have a bandwidth of about 32 GHz. Fig. 10 shows that the THP technique, when coupled with a nonlinearity compensator and post-filter + MLSE, effectively performed better. Fig. 11 shows the BER of the THP + DFE and THP + DFE + post-filter + MLSE structures in case of THP with and without the nonlinearity compensator, at LPF bandwidths of 59, 35, and 30 GHz. At 59 GHz, the compensator entirely lowered the BER to 2.84 × 10^{-3} in the THP + DFE structure and to 2.39 × 10^{-3} in the THP + DFE + post-filter + MLSE structure. At 35 and 30 GHz, on the other hand, when the THP coefficient was fixed at 0.6, the THP + DFE + post-filter + MLSE structure had BERs of 1.32 × 10^{-2} and 3.19 × 10^{-2}, respectively.

Table 1
The computational complexity comparison of the DSP structures.

DSP structures	DFE + MLSE	THP + DFE	THP + DFE + post filter + MLSE
Adder	1176	137	1179
Multiplier	668	147	670

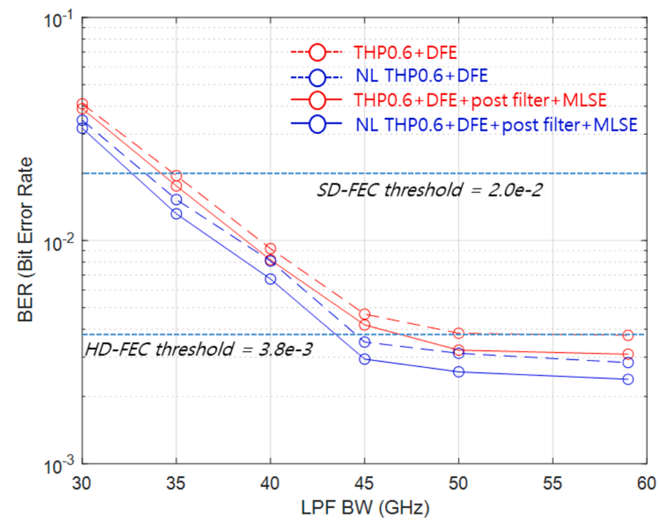

Fig. 10. Relationship between BER and LPF bandwidth in THP + DFE and THP + DFE + post-filter + MLSE, with and without the nonlinearity compensator.

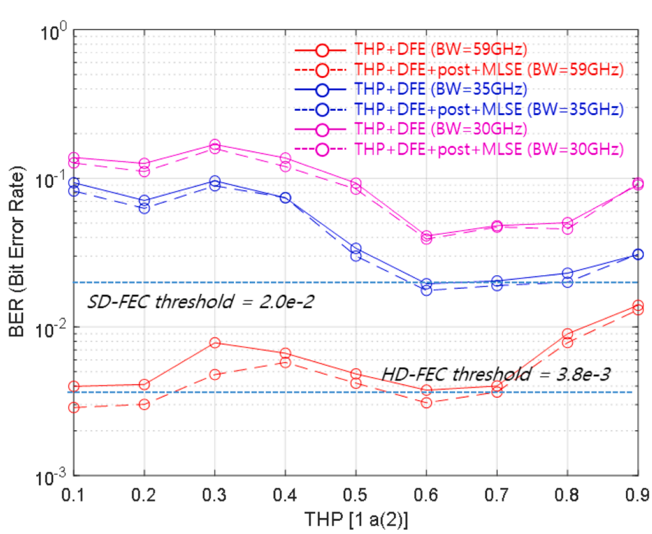

Fig. 9. Relationship between BER and the coefficients of the THP + DFE and THP + DFE + post-filter + MLSE structures at bandwidths of 59, 35, and 30 GHz.

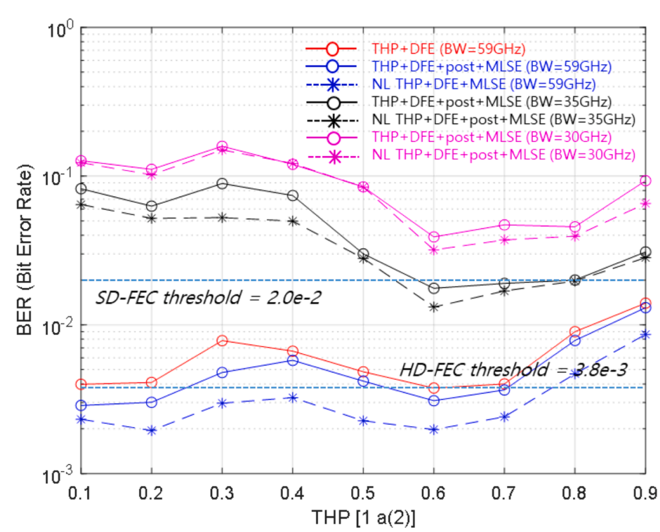

Fig. 11. Nonlinearity compensation with limited bandwidth.

6. Conclusions

We demonstrated the operation of a 200 Gbps, PAM-4 transmission system over 10 km of SMF. By introducing a simple, two-tap THP and by adjusting the DFE feedback coefficient, we avoided the high levels of complexity and compensated for the residual ISI inherent in existing methods. The performances of these systems were analyzed in terms of the BER results according to the ISI mitigation, while changing the THP coefficient. We then compared the BER performances of the THP + DFE, DFE and DFE + MLSE structures under conditions of sufficient and limited bandwidth. When the bandwidth was sufficient, DFE (or DFE + MLSE) satisfied the HD-FEC threshold and THP + DFE, with the optimized THP coefficient of 0.6, had a similar performance to DFE. However, to find out the effects of bandwidth limitations, we add LPF on simulation and varied its bandwidth to demonstrate that SD-FEC limit can be satisfied using a simple two-tap THP and DFE, even when lowered to 35 GHz. Due to ISI mitigation, additional compensation can be made by applying post-filter + MLSE after DFE on the receiver side. Further, the LUT-based nonlinearity compensator for two-tap THP improved the system by enabling 200 Gbps PAM-4 transmission for more than 10 km of SMF. Additional THP with nonlinearity compensator and post-filter + MLSE can lower by 32 GHz of LPF bandwidth for BER to satisfy below the SD-FEC threshold.

CRediT authorship contribution statement

Seung-Woo Lee: Conceptualization, Methodology, Software, Validation, Investigation, Data curation, Writing – original draft, Visualization. **Sang-Rok Moon:** Validation, Writing – review & editing, Supervision. **Hae Young Rha:** Software, Validation, Formal analysis, Writing – review & editing. **Joon Ki Lee:** Supervision, Project administration, Funding acquisition.

Declaration of Competing Interest

The authors declare the following financial interests/personal relationships which may be considered as potential competing interests: Seung-Woo Lee has patent METHOD FOR PRECODING TO MITIGATE NONLINEAR DISTORTIONS AND PRECODER FOR PERFORMING THE SAME pending to Electronics and Telecommunications Research Institute.

Data availability

The authors do not have permission to share data.

Acknowledgement

This work was supported by the Institute of Information & Communications Technology Planning & Evaluation (IITP) grant, funded by the Korean government (MSIT). (No. 2019-0-00002, Development of Optical Cloud Networking Core Technology)

References

[1] X. Li, et al., "102 Gbaud PAM-4 transmission over 2 km using a pulse shaping filter with asymmetric ISI and Tomlinson-Harashima Precoding," OFC 2020, T3I.1.
[2] Q. Hu, et al., Up to 94 GBd THP PAM-4 Transmission with 33 GHz Bandwidth Limitation, ECOC (2018).
[3] T. Wettlin, et al., Beyond 200 Gb/s PAM4 Transmission using Tomlinson-Harashima Precoding, ECOC (2019).
[4] X. Pang, et al., 200 Gbps/Lane IM/DD technologies for short reach optical interconnects, J. Lightwave Technol. 38 (2) (2020).
[5] IEEE Std 802.3bs-2017 IEEE Standard for Ethernet Amendment 10: Media Access Control Parameters, Physical Layers and Management Parameters for 200 Gb/s and 400 Gb/s Operation.
[6] K. Zhong, et al., Experimental demonstration of 500 Gbit/s short reach transmission employing PAM4 signal and direct detection with 25 Gbps device. Proc. Opt. Fiber Communication., Los Angeles, CA, USA, 2015. Paper Th3A.3.
[7] Z. Xing, et al., Experimental demonstration of 600 Gb/s net rate PAM4 transmissions over 2 km and 10 km With a 4- CWDM TOSA, J. Lightwave Technol. 38 (11) (2020).
[8] Q. Hu, et al., "84 GBd Faster-Than-Nyquist PAM-4 Transmission Using Only Linear Equalizer at Receiver," OFC 2019, W4I.2.
[9] M. Xiang, et al., Single-lane 145 Gbit/s IM/DD transmission with faster-than-Nyquist PAM4 signaling, IEEE Photon. Technol. Lett. 30 (13) (2018).
[10] M. Xiang, et al., Experimental study of performance enhanced IM/DD transmissions combining 4D Trellis coded modulation with precoding, Optics Express 26 (25) (2018).
[11] S.R. Moon, et al., C-band PAM-4 signal transmission using soft-output MLSE and LDPC code, Optics Express 27 (1) (2019).
[12] N. Kikuchi, et al., Proposal of LUT-based transmitter nonlinearity compensator with precursor compensation for Short-Reach IM/DD PAM Signalling with Tomlinson-Harashima Precoding (THP), ECOC (2020).
[13] J. Zhang, et al., PAM-8 IM/DD transmission based on modified lookup table nonlinear predistortion, IEEE Photon. J. 10 (3) (2018).